CD133 Expression Correlates with Membrane Beta-Catenin and E-Cadherin Loss from Human Hair Follicle Placodes during Morphogenesis

Denise L. Gay[1,6], Chao-Chun Yang[1,2], Maksim V. Plikus[3], Mayumi Ito[4], Charlotte Rivera[1], Elsa Treffeisen[1], Laura Doherty[1], Michelle Spata[1], Sarah E. Millar[1,5] and George Cotsarelis[1]

Genetic studies suggest that the major events of human hair follicle development are similar to those in mice, but detailed analyses of this process are lacking. In mice, hair follicle placode "budding" is initiated by invagination of Wnt-induced epithelium into the underlying mesenchyme. Modification of adherens junctions (AJs) is clearly required for budding. Snail-mediated downregulation of AJ component E-cadherin is important for placode budding in mice. Beta-catenin, another AJ component, has been more difficult to study owing to its essential functions in Wnt signaling, a prerequisite for hair follicle placode induction. Here, we show that a subset of human invaginating hair placode cells expresses the stem cell marker CD133 during early morphogenesis. CD133 associates with membrane beta-catenin in early placodes, and its continued expression correlates with loss of beta-catenin and E-cadherin from the cell membrane at a time when E-cadherin transcriptional repressors Snail and Slug are not implicated. Stabilization of CD133 via anti-CD133 antibody treatment of human fetal scalp explants depresses beta-catenin and E-cadherin membrane localization. We discuss this unique correlation and suggest a hypothetical model whereby CD133 promotes morphogenesis in early hair follicle placodes through the localized removal of membrane beta-catenin proteins and subsequent AJ dissolution.

Journal of Investigative Dermatology (2015) **135,** 45–55; doi:10.1038/jid.2014.292; published online 14 August 2014

INTRODUCTION

In mice, hair follicle placode induction and early morphogenesis require spacial and temporal activation cues, of which Wnt activation is the earliest known signal. This is followed by activation of EDA/EDAR, transforming growth factor (TGF)-beta, Sonic Hedgehog, and other signaling pathways to prompt organ downgrowth and differentiation (Chiang *et al.*, 1999; Millar, 2002; Mikkola, 2007). The first shape modifications defining the new placode from adjacent interfollicular epidermis include elongation and cell membrane apical curvature promoting invagination of Wnt-activated cells.

Adherens junctions (AJs), required for tight cell–cell contacts, undergo considerable remodeling during skin and hair morphogenesis, and their proteins, in particular E-cadherin and beta-catenin, have been well studied in this regard (Stepniak *et al.*, 2009; Heuberger and Birchmeier, 2010).

E-cadherin down-modulation appears to be a critical event in early ''budding'' morphogenesis, and its downregulation is a well-known early step in hair placode morphogenesis (Müller-Röver *et al.*, 1999; Jamora *et al.*, 2003; Tinkle *et al.*, 2003, 2008). It has been shown that E-cadherin may be down-regulated via one of several mechanisms. First, its transcription can be negatively regulated by Twist and Snail/Slug transcriptional modifiers (reviewed by Peinado *et al.*, 2007), which are in turn targets of Wnt and/or TGF-beta activation (Jamora *et al.*, 2005; ten Berge *et al.*, 2008). Hair follicle budding morphogenesis has been shown to depend upon this pathway in mice, albeit later than the earliest stages of cell curvature and invagination (Jamora *et al.*, 2005, Devenport and Fuchs, 2008). Alternatively, E-cadherin protein can be down-modulated at the cell membrane, and several adhesion proteins and planar polarity proteins, including epithelial cell adhesion molecule (EpCAM), have been implicated in this process, although none has been shown to have a role

[1]*Department of Dermatology, Perelman School of Medicine, University of Pennsylvania, Philadelphia, Pennsylvania, USA;* [2]*Department of Dermatology, National Cheng Kung University Hospital, College of Medicine, National Cheng Kung University, Tainan, Taiwan;* [3]*Department of Developmental and Cell Biology, Sue and Bill Gross Stem Cell Research Center, University of California, Irvine, Irvine, California, USA;* [4]*Department of Dermatology, New York University Langone Medical Center, New York, New York, USA and* [5]*Department of Cell and Developmental Biology, University of Pennsylvania, Philadelphia, Pennsylvania, USA*

[6]*Current address: UMR 967 CEA-INSERM, Fontenay-aux-Roses, France.*

Correspondence: George Cotsarelis, Department of Dermatology, Perelman School of Medicine, University of Pennsylvania, Philadelphia, Pennsylvania 19104, USA. E-mail: cotsarel@mail.med.upenn.edu

Abbreviations: AJ, adherens junction; EMT, epithelial to mesenchymal transition; EpCAM, epithelial cell adhesion molecule; HDAC, histone deacetylase; IF, immunofluorescence; TGF, transforming growth factor

Received 6 January 2014; revised 21 May 2014; accepted 4 June 2014; accepted article preview online 10 July 2014; published online 14 August 2014

in hair follicle budding morphogenesis (Litvinov *et al.*, 1997; Shtutman *et al.*, 2006; Warrington *et al.*, 2013).

Beta-catenin is a component of AJs, linking E-cadherin to the underlying cytoskeleton. Although the relative importance of beta-catenin to AJs during skin development has been directly addressed in conditional beta-catenin knockouts, its role has been difficult to establish because related family member plakoglobin can partially compensate for its loss (Huelsken *et al.*, 2001). Examining a role for beta-catenin in hair follicle development has been further impeded because placode induction requires Wnt activation, of which beta-catenin is an essential component. Thus, knockouts lack even the earliest formation of placodes (Huelsken *et al.*, 2001; Andl *et al.*, 2002; Zhang *et al.*, 2008).

CD133, a pentaspan membrane glycoprotein, is a well-known stem cell marker in hematopoietic and neural tissues, and it is also expressed on progenitor cells and simple luminal epithelia in a number of tissues (Florek *et al.*, 2005; Karbanova *et al.*, 2008). Although widely studied, its function remains unclear (Corbeil, 2013; Grosse-Gehling *et al.*, 2013). Recently, CD133-knockout mice were shown to exhibit reduced mammary gland ductal branching, suggesting a possible role in tube morphogenesis (Anderson *et al.*, 2012). In an unrelated study, it was shown that CD133 can interact with the histone deacetylase 6 (HDAC6) at the cell membrane to reduce membrane beta-catenin and stabilize it via deacetylation for increased Wnt activation in human cells (Mak *et al.*, 2012).

We have found that CD133 is expressed in early human hair follicle placodes, and that its expression correlates with membrane beta-catenin and E-cadherin down-modulation. On the basis of these and related studies, we propose a potential model for AJ disassembly during early human placode morphogenesis through the down-modulation of membrane beta-catenin by CD133.

RESULTS

CD133 expression defines a sub-population of cells in the developing human hair follicle placode

In analyzing the expression of various markers in human epidermis during fetal development (embryonic week 12–14), we found that CD133 (prominin 1) localized to a sub-population (2%) of alpha6-integrin$^+$EpCAM-high basal cells (Figure 1a). In agreement with Ito *et al.* (2007), we found no CD133 expression in embryonic mouse follicular or inter-follicular epidermal cells, indicating that this expression pattern is unique to humans (Supplementary Figure S1 online).

Confocal analyses of 12-week fetal epidermis whole mounts showed that EpCAM and CD133 colocalized on early hair follicle placodes (Figure 1b) (anti-CD133 antibodies AC133 and 293C3 showed identical staining patterns in human fetal scalp (see Supplementary Figure S2 online)). EpCAM expression appeared to precede that of CD133 because EpCAM-only placodes could be observed at this early time point (Figure 1b, left panel), whereas placodes at later times always expressed both markers. Immunofluorescence (IF) analyses of fetal skin cross-sections and confocal image stacks of entire placodes showed that CD133 colocalized with EpCAM along apical and lateral cell–cell boundaries (Figure 1c and d). During hair follicle development, CD133 expression appeared to shift from early basal localization to redistribution along apical and lateral junctions with some retention of the protein at basal junctions in hair germs (Figure 1e). CD133 expression decreased markedly at later times, suggesting that its functions are limited to early placode development.

CD133 expression correlates with Wnt activation and morphogenesis but not proliferation

To precisely delineate the stages of hair follicle development associated with CD133 expression, we compared its localization with a panel of proteins known to be important for mouse placode induction and subsequent morphogenesis (Figure 2a–c). Canonical Wnt activation is an important induction event in mouse hair follicle development (Andl *et al.*, 2002; Zhang *et al.*, 2008). CD133 expression correlated with Wnt activation, as determined by translocation of beta-catenin to nuclei and expression of Wnt target LEF1 in early human hair follicle placodes (Figure 2a, top panels). Key morphogenetic regulators, TGF-beta and Wif1, were also observed in CD133$^+$ cells (Figure 2a; Jamora *et al.*, 2005; Surmann-Schmitt *et al.*, 2009).

Surprisingly, Ki-67, a nuclear marker for proliferating cells, only infrequently colocalized with CD133-expressing cells in early placodes (Figure 2a). Triple staining for Ki-67, CD133, and Lef1 confirmed that early placodes had undergone Wnt activation but remained relatively quiescent (Figure 2c and d for quantification).

Early budding morphogenesis is characterized by AJ remodeling and E-cadherin down-modulation, allowing for cell movement and shape changes concurrent with invagination. In agreement with studies on murine hair follicle morphogenesis (Müller-Röver *et al.*, 1999), E-cadherin was downregulated and a related cadherin, p-Cadherin, was upregulated at this time point (Figure 2a).

Snail, an important downregulator of E-cadherin transcription, was not found in early placodes (Figure 2a and b and Supplementary Figure S3 online), although, in agreement with previous reports (Jamora *et al.*, 2005; Devenport and Fuchs, 2008), hair germs expressed activated nuclear Snail (Figure 2b). Slug, a close relative of Snail also implicated in E-cadherin transcriptional regulation (Bolos *et al.*, 2003), was present in the cytoplasm of many basal cells including early placodes; however, nuclear localization of activated Slug was rare (Figure 2a and b and Supplementary Figure S3 online). Thus, down-modulation of membrane E-cadherin did not appear to result from transcriptional repression by Snail/Slug family members.

Transmission electron microscopy analyses confirmed the existence of many gaps at apical and lateral cell–cell junctions along invaginating basal cells within placodes, supporting the concept that these cells are actively engaged in junctional remodeling (Figure 2e). Other reports, examining desmosomal systems in early mouse placodes, also showed a paucity of placode but not interfollicular desmosomes, further supporting this concept (Nanba *et al.*, 2000).

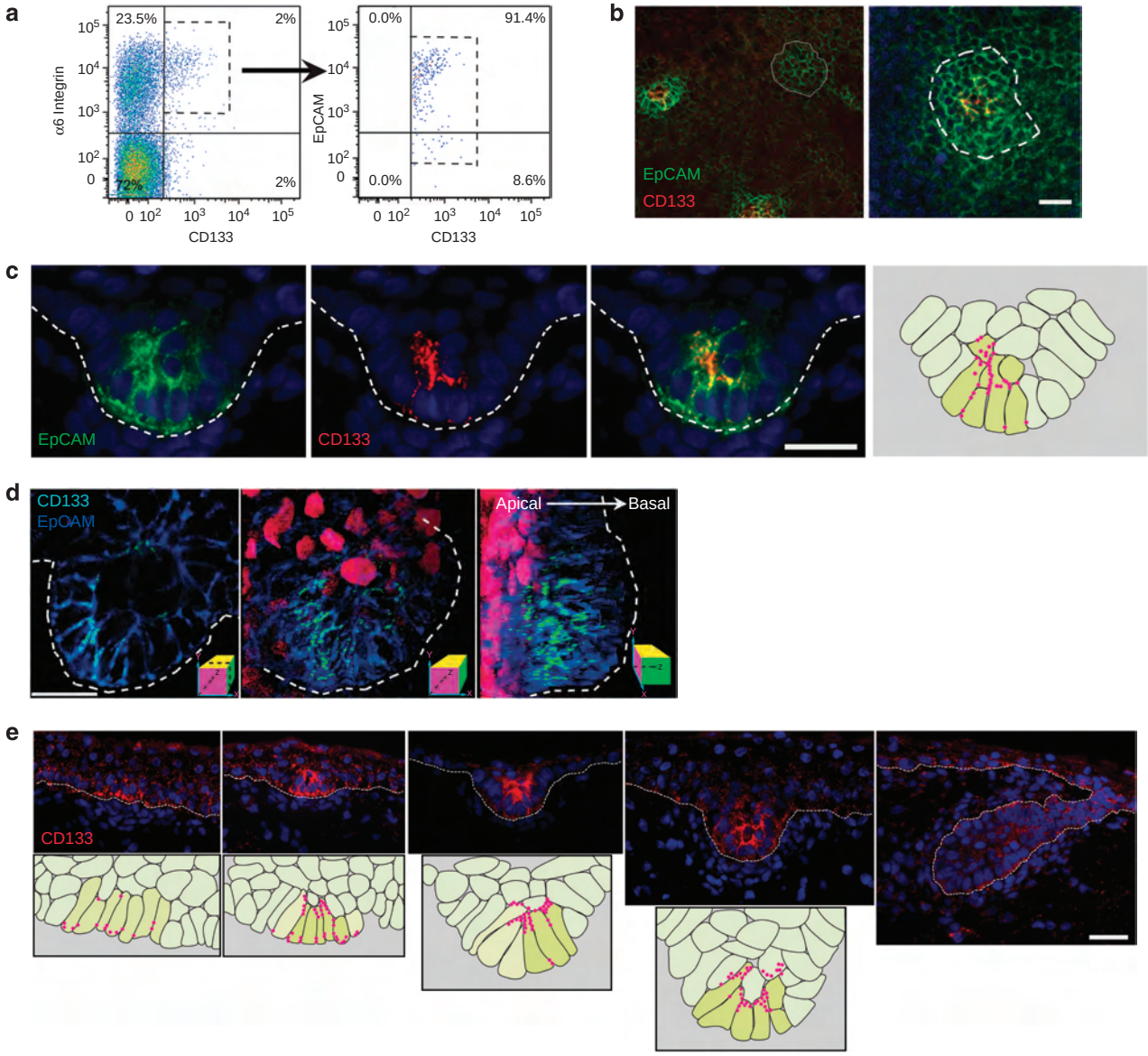

Figure 1. CD133 is an early marker of human hair follicle placodes. (**a**) Density dot plots of fetal scalp epidermal cells for the expression of CD133 and alpha6-integrin (left) and alpha6-integrin$^+$CD133$^+$ cells for epithelial cell adhesion molecule (EpCAM) and forward scatter (right). (**b**) Scalp whole mounts stained for EpCAM and CD133. Dotted line outlines CD133$^-$EpCAM$^+$ placode (left) or magnified CD133$^+$EpCAM$^+$ placode (right). (**c**) Frozen section of placode stained for EpCAM, CD133, overlap, or schematic of CD133 localization. 4′,6-Diamidino-2-phenylindole (DAPI)-stained nuclei are blue. Schematic placode cells are shaded light yellow (CD133$^-$ cells) and dark yellow (CD133$^+$ cells). The red dots represent CD133 location. (**d**) Single (left) and 3D-stacked confocal images (middle and right) of placode stained for EpCAM and CD133. Drawings denote orientation. Light purple nuclei in the middle and right panels show DAPI-stained periderm. (**e**) Developing hair follicles analyzed for CD133 expression with schematic representations below. Scale bars are 25 μm. (**a**–**e**) $N = 12$ and N(t) = 6 (where N indicates the number of times these experiments were performed and N(t) = number of individual tissue samples analyzed).

CD133$^+$ cells express genes implicated in early hair follicle placode morphogenesis and related epithelial to mesenchymal transition (EMT)

To better define the role of CD133$^+$ cells in placode development, 13-week fetal scalp epidermal cells were sorted for the expression of CD133 and alpha6-integrin (Figure 3a) and RNA was subjected to microarray analyses. As expected, alpha6-integrin$^+$CD133$^-$ (ITGA6$^+$) and α6-integrin$^+$CD133$^+$ double-positive (CD133$^+$) populations, both of epidermal basal origin, shared the expression of many genes (Figure 3b, Venn diagram). Figure 3c shows a heatmap comparing differences in gene expression by ITGA6$^+$ and CD133$^+$ populations.

As anticipated, multiple activation pathways were upregulated in the CD133$^+$ population, in agreement with those previously defined as important for murine hair follicle development (Table 1; Millar, 2002; Lee and Tumbar, 2012). Independent bioinformatics analyses also revealed upregulation of overlapping gene sets in the CD133$^+$ population

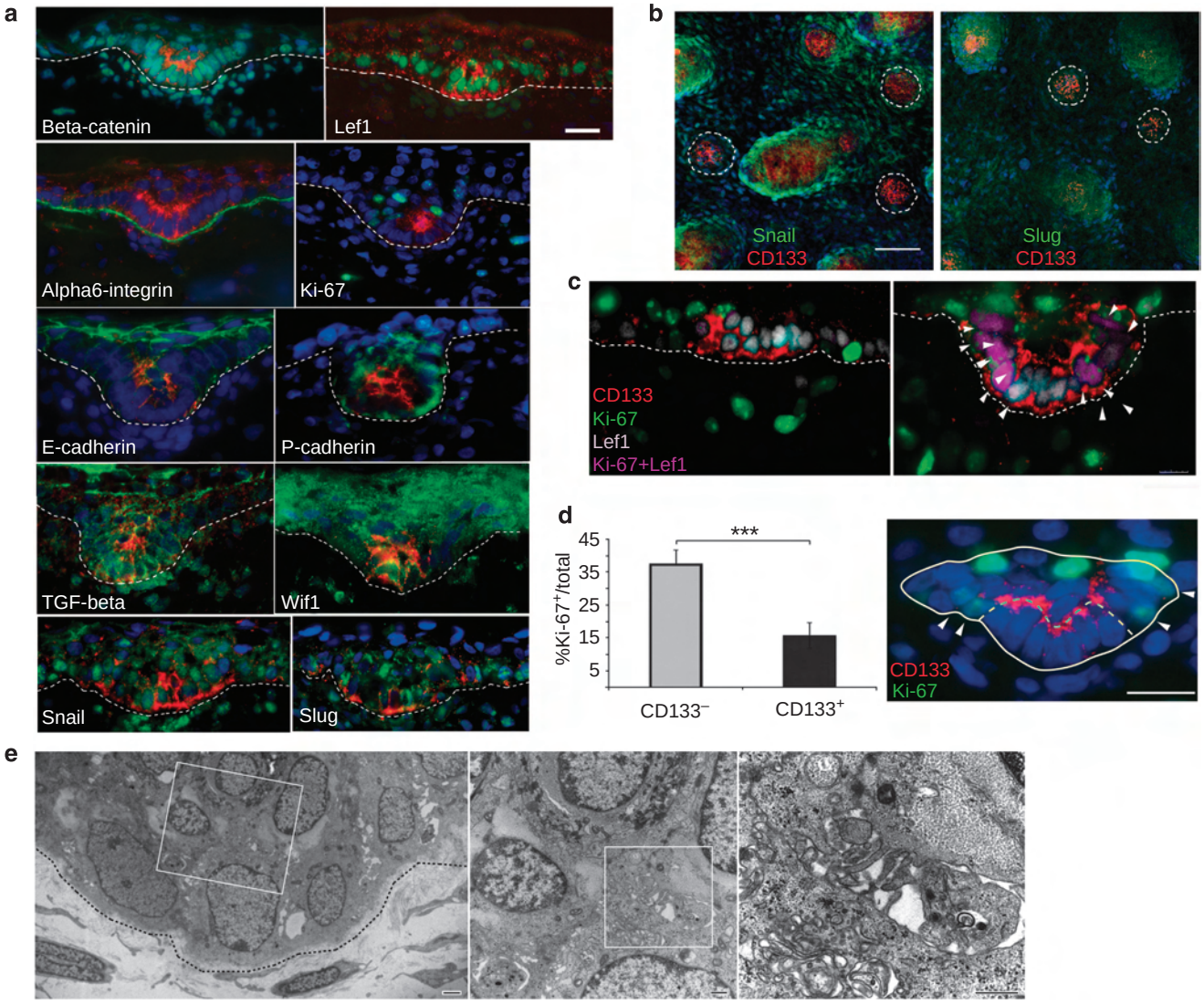

Figure 2. CD133 expression correlates with Wnt activation and early hair morphogenesis, but not proliferation. (**a**) Frozen sections of placodes costained for CD133 (red) and labeled markers (see panels). 4′,6-Diamidino-2-phenylindole (DAPI)-stained nuclei are blue. Scale bar = 25 μm. (**b**) Stacked confocal images of fetal scalp epidermis whole mounts stained for Snail or Slug and CD133. White dotted lines outline placodes. Scale bar = 75 μm. (**c**) Triple staining of frozen sections for CD133, Lef1, and Ki-67. White arrows denote locations of Lef1:Ki-67 double-positive cells (right). Scale bar = 25 μm. (**a**–**c**) *N* and N(t) = 3. (**d**) Bar graph comparing percent Ki-67$^+$ cells within CD133$^-$ and CD133$^+$ populations. Data are means ± SEM, ***P < 0.005. Example of compared regions (right). Arrows indicate Ki-67$^+$ cells adjacent to CD133$^+$ cells. Scale bar = 25 μm. N = 22 placodes analyzed and N(t) = 3. (**e**) Transmission electron microscopy (TEM) analysis of 12-week placode. Rectangles show areas of magnification from left to right. Scale bars: left = 2 μm; others = 500 nm. *N* and N(t) = 4.

associated with morphogenesis and related EMT functions, in particular those associated with signaling and cell motility. In addition, genes associated with cell–cell adhesion were downregulated. Interestingly, no known EMT transcriptional modifier of e-cadherin was upregulated, and targets of these modifiers were not downregulated, including CDH1, CDH2, vimentin, and fibronectin, in the CD133$^+$ population (Table 1).

Array analyses and quantitative real-time polymerase chain reaction of ITGA6$^+$ and CD133$^+$ populations (Supplementary Table 1 online and Figure 3d) confirmed IF data (Figure 2a) that CD133$^+$ cells had undergone Wnt activation and served as a primary source of TGF-beta2, Wif1, and Slug (SNAI2) transcription. As mentioned above, CDH1 (e-cadherin) gene expression was not downregulated (Table 1), although protein expression was clearly downregulated in CD133$^+$ cells (Figure 2a). Quantitative real-time polymerase chain reaction confirmed that Snail (SNAI1) transcription was essentially absent from CD133$^+$ cells, whereas Slug (SNAI2) was expressed by both ITGA6$^+$ and CD133$^+$ populations (Figure 3d). Observations that inactive Slug localized to the cytoplasm rather than the nucleus in IF analyses (Figure 2a and b and Supplementary Figure S3 online) were supported by the fact that Slug-downregulated gene targets such as CLDN1 were upregulated in CD133$^+$ cells (Table 1; Martínez-Estrada *et al.*, 2006).

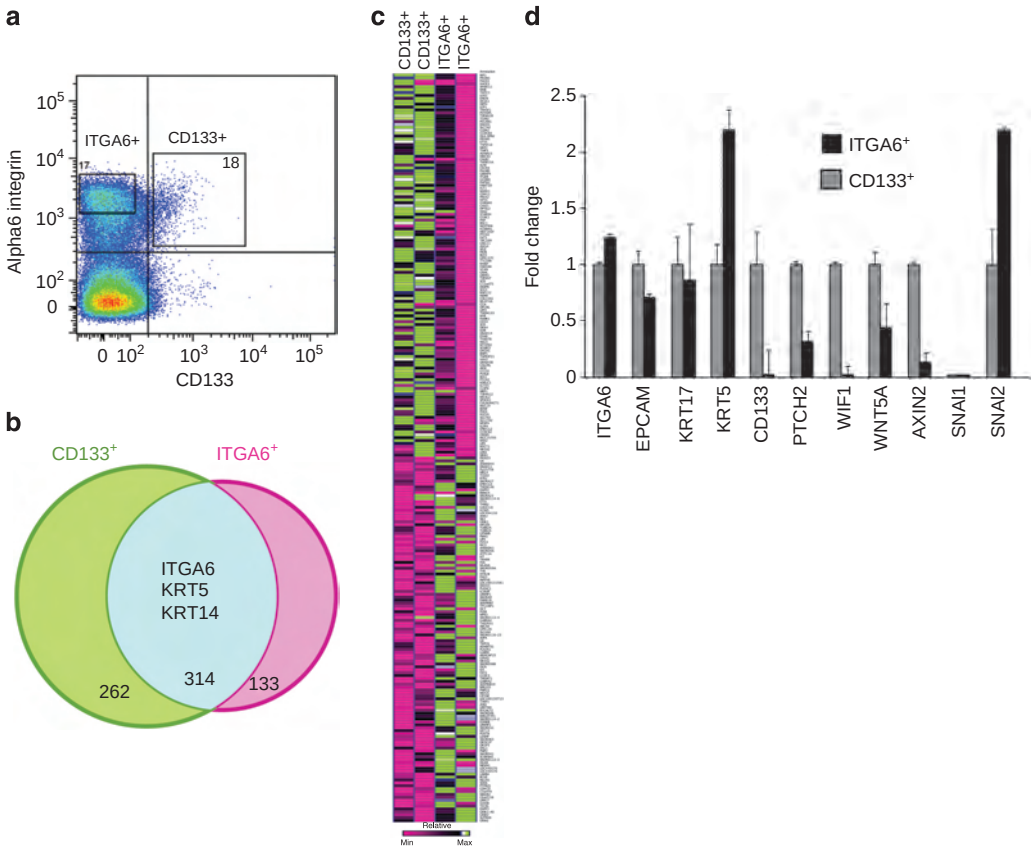

Figure 3. CD133$^+$ cells express genes indicative of early hair follicle placode morphogenesis and epithelial to mesenchymal transition (EMT). (**a**) Representative dot plot of 13-week fetal scalp epidermal populations. Squares define regions of ITGA6$^+$ and CD133$^+$ sorted populations. (**b**) Venn diagram comparing overlap of gene expression in ITGA6$^+$ and CD133$^+$ populations. (**c**) Heatmap comparing differentially expressed genes in ITGA6$^+$ and CD133$^+$ populations from two independent array analyses. Green denotes upregulated genes and pink denotes downregulated genes. *N* and N(t) = 2 arrays from two independent sorts. Results represent merged analyses. (**d**) Quantitative real-time polymerase chain reaction (QPCR) analyses comparing transcription levels of specific genes in sorted ITGA6$^+$ (black bars) and CD133$^+$ (gray bars) populations, as described in Gay *et al.*, 2013. *N* and N(t) = 3.

These combined results suggest that, although CD133$^+$ cells engage in budding morphogenesis and express downstream genes associated with this (and shared with EMT-mediated morphogenesis), EMT regulators do not initiate this event.

CD133 colocalizes with AJ proteins in early hair placodes and localizes to regions with decreased membrane beta-catenin and E-cadherin in more mature placodes

To investigate whether CD133 localized specifically to cell–cell junctions, fetal scalp epidermis was subjected to brief trypsinization and mechanical disruption to disengage placode and subplacode clusters from surrounding interfollicular epidermis for more detailed viewing. CD133 colocalized with EpCAM along cell membranes and appeared to localize specifically to cell–cell junctions (Figure 4a).

To determine which types of junctions CD133 might associate with, we undertook IF analyses. CD133 clearly localized to areas rich in E-cadherin during early placode curvature and, later, localized specifically to regions with downregulated E-cadherin expression (Figure 4b). In contrast, CD133, as has been previously reported for EpCAM (Lei *et al.*, 2012; Wu *et al.*, 2013), did not localize to tight junctions, as determined by ZO1 costaining (Figure 4c).

CD133 has been reported to coassociate with HDAC6 and beta-catenin proteins at cell membranes (Mak *et al.*, 2012). As membrane beta-catenin is an essential constituent of AJs, we studied whether CD133 colocalized with beta-catenin on placode cell membranes. IF confirmed their colocalization during early placode morphogenesis (Figure 4d). We also confirmed that HDAC6 is broadly expressed in the cytoplasm of epidermal cells and specifically colocalizes with CD133 along cell membranes (Figure 4e).

To establish that CD133 associates with specific membrane proteins, and because co-immunoprecipitation analyses would be difficult given the low percentage of CD133$^+$ cells in fetal epidermis, *in situ* proximity ligation assay technology was used. Proximity ligation assay analyses supported the idea that CD133 protein specifically bound EpCAM, beta-catenin, and HDAC6 but not E-cadherin in placodes (Figure 4f, red dots correspond to areas of specific protein–protein interaction. See Supplementary Figure S4 online for negative single antibody staining). Additional IF analyses to independently locate beta-catenin or HDAC6 and CD133 further confirmed

Table 1. Microarray results of differentially regulated and unaffected genes in CD133$^+$ cells compared with ITGA6$^+$ cells

	CD133$^+$ population: upregulated genes
Signaling pathways: target genes	**WNT**: WIF1, DKK4, LGR5, WNT5A **SHH**: PTCH2 **EDA/EDAR**: EDAR **TGF**: TGFB2, BMP5 **Others**: BDNF, FGF20, TNFS10
Cell motility and morphogenesis (DAVID[1])	CD34, VAV3, SELE, CXCR4, DCLK1, FLT1, KDR, NRP1, NRP2, TGFB2, VCAN, BDNF, KIF5C, LIFR
Downstream targets of EMT (signaling pathways, cell motility, and unknown functions) (Groger *et al.*, 2012[2]; Humtsoe *et al.*, 2012; Byers *et al.*, 2013)	TGFB2, WNT5A, ETV5, VCAN, NRP2, ADAM23, CLD1, A2M, HAS2, GNG11, MSX2, SCUBE3, MYB, MCCT1, NRSA2, BDNF, NRP1, VAV3 FRZB, CDH11, PAPSS2, SLC27A2
Mammary stem cell gene set (GSEA M2573)	PRDM1, WIF1, LIFR, DUSP6, NRP1, GNGL1, MICAL2, NRP2, COL14A1, MME, ETV5, KCNMA1, HAS2, MYB, LRRN1, KDELC1
	CD133$^+$ population: unaffected genes
EMT down-modulators of E-cadherin (Lamouille *et al.*, 2014)	SNAI1, SNAI2, ZEB1, TCF3, TCF4, KLF8, TWIST, SIX1, FOXC2, FOXF1, FOXD3, FOXQ1, FOXA1, FOXA2, GATA4, GATA6, HMGA2, ZNF703, PRX1
Downregulated genes during EMT (Lamouille *et al.*, 2014)	GRHL2, ELF3, ELF4
EMT targets (Lamouille *et al.*, 2014)	CHD1, CDH2, FN1, VIM
	CD133$^+$ population: downregulated genes
Adhesion and cell junctions (DAVID)	FAT2, CDH19, LAMB4, GPNMB, LSAMP, NRXN1, POSTN, PLXNC1, DSG1, EPB4IL3, FMN1, GABRA2, GABRA4, GABRE, GRIA2, GRID2, GRIK1, LRRC7, PMP22, NLGN1
Gated channel activity (DAVID)	Gabra2, Gabra4, Gabre, gria2, Grid2, Grik1, Nmur2, Kcnj5, Ryr2, Trpc6
Pigmentation (DAVID)	DCT, EDNRB, PAX3, KIT, TYR, TYRP1
EMT down-modulators of E-cadherin (Lamouille *et al.*, 2014)	ZEB2

Abbreviations: DAVID, database for annotation, visualization and integrated discovery; EMT, epithelial to mesenchymal transition.
[1]Bioinformatics programs and references are defined in Materials and Methods section.
[2]References are provided in left column in parentheses.

these observations (Figure 4f); however, the low incidence of CD133–HDAC6 interaction suggested that it may be transient.

CD133 has been implicated in loss of beta-catenin from cell membranes (Mak *et al.*, 2012). As beta-catenin is highly abundant in the epidermis, potential changes in its membrane expression might not be detected by conventional IF microscopy. To analyze this, confocal microscopy of whole placodes costained for CD133, E-cadherin, and beta-catenin was undertaken. Figure 4g shows a typical early placode, with some CD133–beta-catenin colocalization (pink arrowhead). However, overall, CD133-rich membranes exhibited decreased beta-catenin localization (Figure 4g, white arrowheads). Quantification of the levels of beta-catenin along CD133-positive and CD133-negative membranes confirmed this observation (Figure 4h). Tight localization of E-cadherin to cell junctions, which could be easily observed in CD133-negative regions, was also lost (Figure 4g, right panels, white arrowheads).

To analyze CD133 protein localization in detail, silver enhanced gold-particle IF transmission electron microscopy analyses were undertaken. Initial IF analyses showed good labeling of anti-CD133-treated placodes and thus good penetration into tissue (Supplementary Figure S5 online). IF transmission electron microscopy analyses showed specific localization of gold particles to regions typically rich in AJs, near or in gaps along lateral and apical cell–cell junctions (Figure 4i). Immunogold also localized infrequently to intracellular vesicles, suggesting that CD133 expression is regulated via endosomal trafficking (Figure 4i).

Anti-CD133 antibody increases the down-modulation of cell membrane beta-catenin and E-cadherin in human fetal scalp explants

To directly address a function for CD133, we studied fetal scalp explants (Figure 5a for schematic and Materials and Methods section for culture details and potential caveats). Explants cultured for 16–20 hours retained good morphology and development, as evidenced by continued follicle growth (Figure 5b); however, at later times, epidermal structure became disorganized.

The unavoidable short culture duration prevented us from undertaking knockdown experiments with small interfering RNAs or viruses to address long-term effects such as morphologic or transcriptional alterations. Therefore, explants were cultured for a short term with anti-CD133 antibodies to address potential changes in membrane E-cadherin and

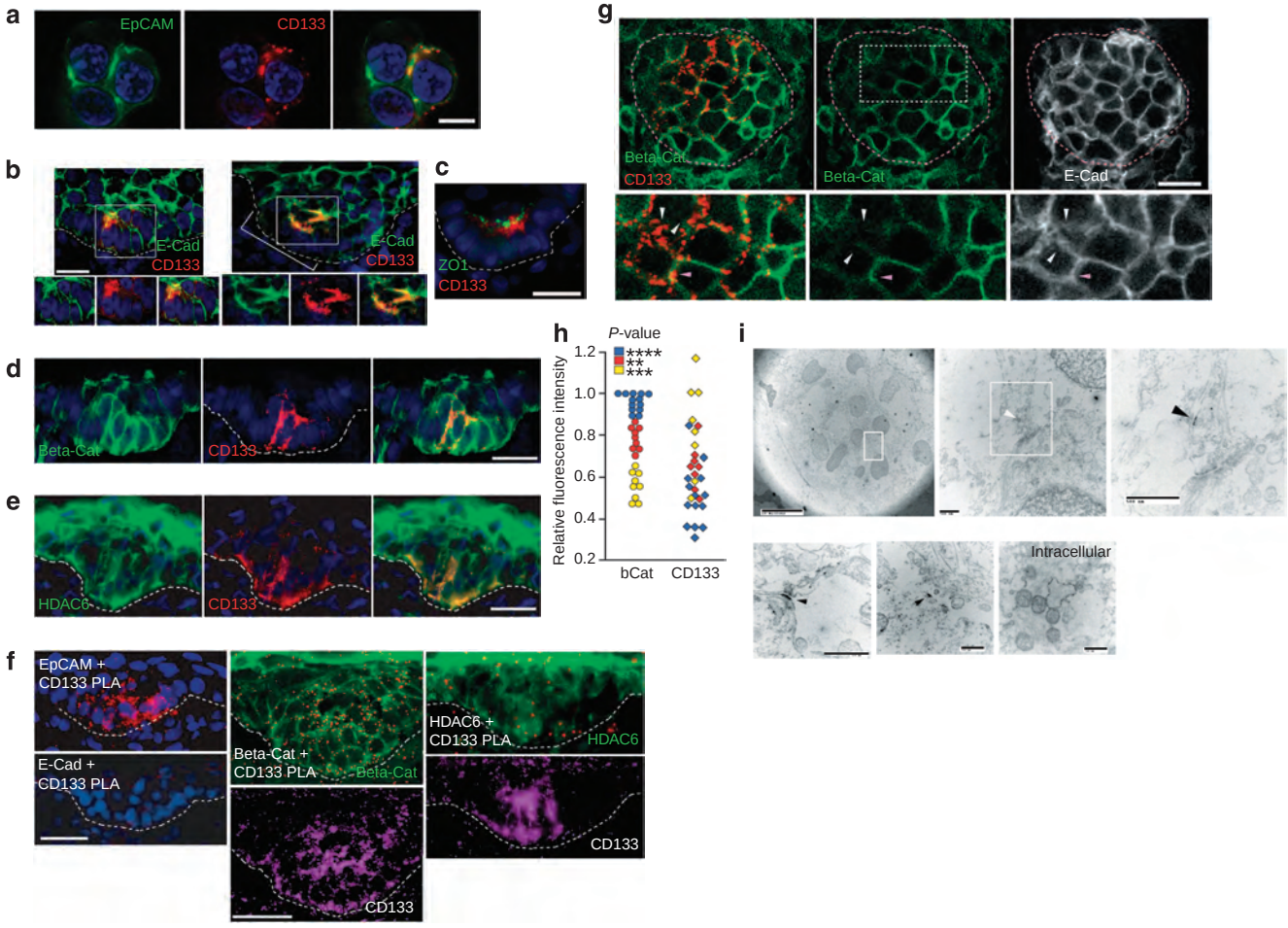

Figure 4. CD133 localizes to adherens junctions (AJs) in early placodes and to regions of beta-catenin and E-cadherin downregulation in later placodes. (**a**) Immunofluorescence (IF) image of subplacode cluster, dissociated from surrounding interfollicular epidermis, stained for CD133 and epithelial cell adhesion molecule (EpCAM). Scale bar = 5 μm. (**b**) IF images of early (left) and later (right) placodes stained for CD133 and E-cadherin. Line (right panel) indicates E-cadherin-depleted region. Squares indicate magnified areas (lower panels). (**c**–**e**) IF of placode stained for CD133 and ZO1 (**c**), beta-catenin (**d**), and HDAC6 (**e**). (**f**) *In situ* proximity ligation assay (PLA) of ''CD133 + EpCAM'', ''CD133 + E-cadherin'', ''CD133 + beta-catenin '', and ''CD133 + HDAC6'' antibody combinations. Placodes in the middle and right panels were counterstained for beta-catenin or HDAC6, respectively, and CD133. Scale bars = 25 μm in (**b**–**f**). (**g**) Stacked confocal images of a placode costained for CD133, beta-catenin, and E-cadherin. Rectangle defines magnified regions (lower panels). White arrowheads indicate regions of high CD133 and low beta-catenin and E-cadherin localization. Pink arrowhead indicates colocalized proteins. Scale bar = 10 μm. (**h**) Scatter plot comparing relative fluorescence intensities of beta-catenin and CD133 proteins along placode cell membranes. Left side shows relative fluorescence of membranes for beta-catenin (bCat): blue (high), red (intermediate), and yellow (low). Right side compares CD133 fluorescence within each group. See Supplementary Figure S6 online for details. $N = 31$ regions from 8 placodes. N(t) = 3. $^{**}P < 0.01$, $^{***}P < 0.005$, $^{****}P < 0.001$. (**i**) Immunofluorescence transmission electron microscopy (IFTEM) of CD133 localization in placodes. Boxed regions show increased magnification from left to right. Bottom panels provide additional examples. Arrowheads point to regions with high immunogold content. Scale bar: middle left panel = 10 μm; all other panels = 500 nm. (**a**–**i**) *N* and N(t) ⩾ 3.

beta-catenin expression. Anti-CD133 antibody or an isotype control antibody was applied to explants at day 0 and explants were analyzed at 20 hours. Comparison of anti-CD133-treated and control explants showed that anti-CD133 antibody permeated well into placodes during the culture period (Figure 5c). In addition, comparisons of day 0 placodes and anti-CD133 explant placodes showed that antibody treatment over time resulted in increased CD133 surface expression, suggesting that antibody binding prevented CD133 protein internalization (Figure 5c and d).

Explants were analyzed for the expression of membrane E-cadherin protein. Surprisingly, anti-CD133 explant placodes showed markedly reduced E-cadherin expression throughout the entire placode compared with controls (Figure 5e and f for quantification).

Infrequently, placodes that had received less CD133 antibody during culture were observed. These placodes resembled those treated with control antibody, whereas placodes with increased CD133 antibody binding showed dysregulated EpCAM localization, as well as reduced membrane E-cadherin expression (Figure 5g).

Stacked confocal images further demonstrated the differences between anti-CD133-treated and control explants in both EpCAM and E-cadherin localization (Figure 5h, lower left panel was enhanced to show membrane localization of E-cadherin. Insets show unenhanced views). As anticipated,

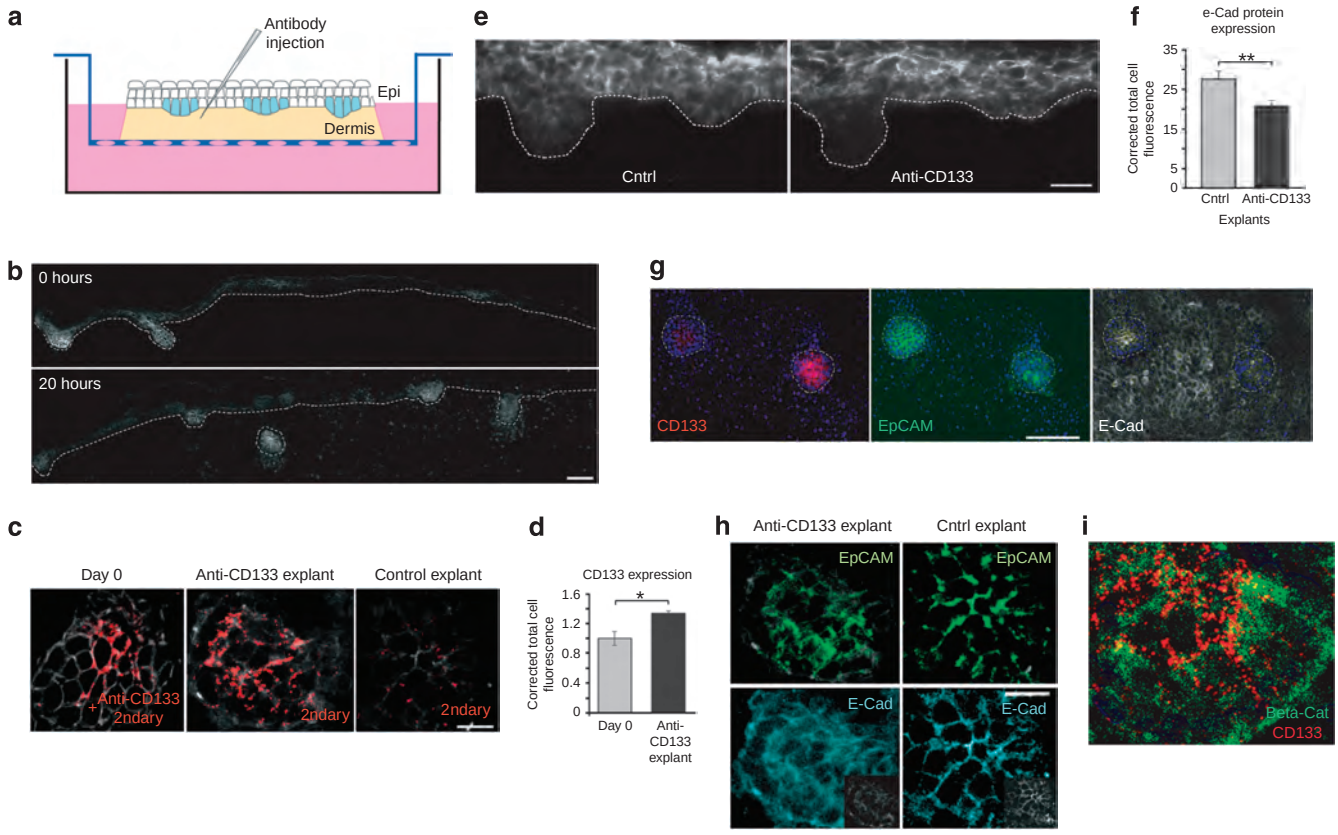

Figure 5. Perturbation of CD133 protein drives accelerated E-cadherin membrane loss in scalp explant placodes. (**a**) Schematic depicting scalp explant. (**b**) Immunofluorescence (IF) images of day 0 (top) and 20-hour explant (bottom) stained for epithelial cell adhesion molecule (EpCAM). Scale bar = 50 μm. (**c**) Confocal images comparing day 0 scalp (stained with anti-CD133 and secondary antibodies, left panel) with anti-CD133 (middle) and control (right) explants stained with secondary antibodies only. (**d**) Bar graph showing relative CD133 protein concentration in day 0 and anti-CD133 explant placodes and germs. $N = 9$ placodes for each group. (**e**) IF of Cntrl and anti-CD133 explants stained for E-cadherin. Scale bar = 25 μm. (**f**) Bar graph showing quantitative comparison of E-cadherin in control and anti-CD133 explant placodes and germs. $N = 18$ placodes for each group. (**g**) Confocal image of adjacent placodes in anti-CD133 explant stained with secondary (CD133, red), EpCAM, and E-cadherin antibodies. Scale bar = 75 μm. (**h**) Confocal images of placodes from anti-CD133 and Cntrl explants stained for EpCAM (top) and E-cadherin (bottom). Insets in E-cad panels show true unenhanced intensities. (**i**) Confocal image from an anti-CD133 explant stained with secondary (red) and beta-catenin antibodies. Scale bars = 10 μm (**c**, **h**, **i**). Data are means ± SEM, $*P<0.05$, $**P<0.01$. (**a**–**i**) N and $N(t) \geqslant 3$.

examination of beta-catenin in anti-CD133 explants showed extensive loss of beta-catenin from membranes specifically in regions of CD133 localization (Figure 5i).

DISCUSSION

Here, we have observed a striking correlation between localized CD133 expression and down-modulation of AJ proteins during human hair follicle placode morphogenesis. CD133 is expressed on the apical and lateral cell membranes of a sub-population of invaginating basal cells during early placode morphogenesis. CD133 physically associates with membrane beta-catenin, and its localization correlates specifically with loss of membrane beta-catenin and E-cadherin in later placodes. Anti-CD133 antibody treatment augments this loss presumably through stabilization of CD133 protein. Given its temporal and regional localization in early placodes and its enhanced function in anti-CD133 explants, we have proposed a hypothetical model suggesting that CD133 may be involved in the down-modulatation of membrane beta-catenin for the destabilization of AJs during early human hair follicle morphogenesis (see model, Figure 6).

Our model supports the concept that CD133 functions primarily during stage I placode formation, that is, after Wnt and Eda–Edar signaling but before induction of e-cadherin transcriptional regulators (Millar, 2002; Schneider *et al.*, 2009). We found no role for Snail or Slug during the earliest steps in human placode morphogenesis. However, activated nuclear Snail and Slug were observed in more differentiated hair germs, as previously reported in mice (Jamora *et al.*, 2005; Devenport and Fuchs, 2008). Therefore, we suggest that the first step in AJ disruption in human placodes at least may be at the level of membrane E-cadherin protein down-modulation, followed by Snail/Slug-mediated E-cadherin transcriptional downregulation. Snail/Slug family members are target genes of Wnt and TGF-beta pathways (Jamora *et al.*, 2005; ten Berge *et al.*, 2008), and indeed Slug expression was evident in early human placodes. However, nuclear localization, indicating activation, was rare. We

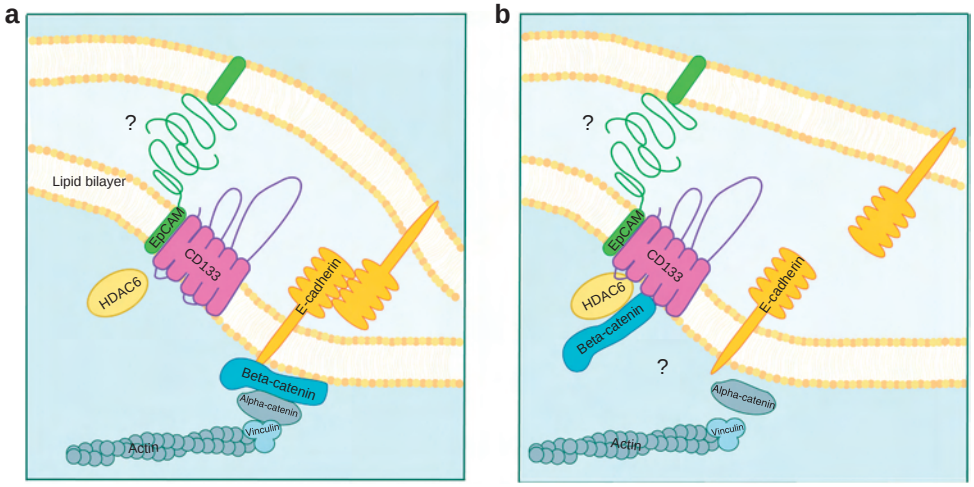

Figure 6. Hypothetical model for the role of CD133 in adherens junction (AJ) loss during human hair follicle placode morphogenesis. (**a**) Schematic representation of an AJ connecting intercellular membranes. (**b**) Proposed model of AJ disruption following CD133 association with AJ beta-catenin protein. It should be noted that CD133 colocalization with AJ proteins before their loss in CD133-rich regions (Figure 4) indicates a time lag that may point to a more complex phenomenon than the simple model proposed here. Epithelial cell adhesion molecule (EpCAM) association with CD133 and possible transient association of HDAC6 with CD133 reflect results from proximity ligation assay analyses in Figure 4. Weak homophilic intercellular interaction between EpCAM proteins has been demonstrated by Litvinov *et al.*, 1994. The question marks for EpCAM–EpCAM interaction (panel **a**) and CD133 sequestration of membrane beta-catenin (panel **b**) denote that these possibilities remain hypothetical.

suggest that requisite cues for Snail/Slug activation may be limiting during this early period.

Whether CD133 participates with HDAC6 in the deacetylation of beta-catenin remains unknown, but CD133 and HDAC6 do coassociate in early placodes, suggesting this as a possibility. Mak *et al.* (2012) showed that HDAC6-mediated beta-catenin deacetylation can upregulate Wnt activity and subsequent proliferation in cell lines. We have not observed proliferation of $CD133^+$ cells in early human placodes; however, $CD133^+$ cells have undergone at least some Wnt activation, as evidenced by nuclear localization of beta-catenin and gene expression of Wnt targets. This suggests that either a threshold of activity has not been met for proliferation or that Wnt activity may not lead to proliferation of these cells. Recent work by Hirata *et al.* (2013) has demonstrated that high levels of Wnt activation can result in the maintenance rather than the proliferation of colonic epithelial stem cells.

Proximity ligation assay analyses showed that CD133 and EpCAM proteins directly associate and may have linked functions. This is not surprising given that they are found on many of the same cells including luminal epithelial precursors and stem cells (Karbanova *et al.*, 2008; Trzpis *et al.*, 2008). In early reports, EpCAM was postulated to directly influence E-cadherin expression and AJ stability in transfected cell lines (Litvinov *et al.*, 1997). In agreement with recent reports, we do not find a direct role for EpCAM in E-cadherin regulation in human hair follicle placodes (Lei *et al.*, 2012; Wu *et al.*, 2013). EpCAM is broadly expressed throughout the placode rather than specifically in regions of E-cadherin downregulation, and its aggregation in anti-CD133 explants does not correlate with E-cadherin and beta-catenin loss.

In these studies, we have shown that humans and mice exhibit many similarities and some differences in hair follicle placode morphogenesis. Wnt activation and later signaling pathways appear to be common to both. However, CD133 is expressed only in human hair follicle placodes, indicating that its function is unique to human hair development. Thus, our results underscore the significant differences that can exist between humans and other mammals and stress the importance of human models.

MATERIALS AND METHODS

Human tissue procurement

Human fetal scalp was procured from Advanced Bioscience Resources (ABR, Alameda, CA) in conformity with federal and state laws and following National Institute of Health Human Fetal Tissue Research Review Panel of 1988 guidelines. The gestation period was estimated by ABR based on testimonials and patient examination. We further distinguished age based on placode coverage (no placodes denoted tissue <11 weeks, partial placode coverage 11–12 weeks, and complete coverage 13 weeks and older). Any observance of external hair shafts defined the tissue as at least 14 weeks.

Prom1 mice

Engineered mice containing a knockin of the creERT2-IRES-nlacZ cassette into the *Prominin 1* locus were kindly provided by Liqin Zhu and Richard Gilbertson (Zhu *et al.*, 2009). Staining of mouse skin for beta-galactosidase expression is as described by Gay *et al.* (2013).

Antibodies

See Supplementary Table 1 online.

Epidermal cell isolation, flow cytometry, and cell sorting

Epidermal cells were isolated using dispase II (Roche, Basel, Switzerland) at 4 °C for 12 hours, followed by treatment with 0.25% trypsin/EDTA for 5 minutes. 4′,6-Diamidino-2-phenylindole was used to exclude dead cells from analyses and sorting. We undertook FACS analyses using a FACSCanto A and cell sorting using a FACSVantage

SE and FACSDiVa software and analyzed data with FlowJo software (BD Biosciences, Piscataway, NJ). Populations were sorted directly into Trizol LS (Life Technologies, Carlsbad, CA) for RNA isolation.

Immunohistochemistry

Briefly, frozen tissue sections were processed as described in Gay *et al.*, 2013. Images were obtained using a Zeiss LSM 710 Confocal (Oberkochen, Germany) or Leica deconvoluting microscope (Wetzlar, Germany) and analyzed using Fiji software (Abramoff, *et al.*, 2004). Fluorescence intensities of individual cell membranes (Figure 4h) were obtained by averaging plot profile lists using the Fiji software (see Supplementary Figure S6 online for a representative analysis). Relative intensities were generated by setting the highest beta-catenin intensity for each placode to 1 and comparing data within and between placodes. In Figure 5d and f, fluorescence intensities of entire placodes were compared.

Detailed immunohistochemistry procedures can be found in Supplementary Methods online.

In situ proximity ligation assay

Frozen tissue sections were treated as for immunohistochemistry (see Supplementary Methods online) by using the following antibody combinations: anti-CD133/2 (1:200) and anti-EpCAM (1:2,500) or anti-E-cadherin (1:4,000), anti-CD133 C-term (1:400), and beta-catenin (1:15,000) or HDAC6 (1:1,000), and further processed as recommended by the manufacturer (Duolink *In Situ*-Fluorescence, Sigma-Aldrich, St Louis, MO).

Micoarray and quantitative real-time polymerase chain reaction analyses

RNA isolation and quantitative real-time polymerase chain reaction were undertaken as previously described (Gay *et al.*, 2013). Microarray services were provided by the University of Pennsylvania Molecular Profiling Facility using the GeneChip Human Gene 1.0 ST Array (Affymetrix, Santa Clara, CA), as described in the Ambion WT Expression Manual. A GeneChip 3000 7G scanner (Affymetrix) was used to collect fluorescence signals. The results in Table 1 reflect combined results from two independent sorts.

Partek Genomics Suite (Partek, St Louis, MO) and GENE-E data analyses software (http://www.broadinstitute.org/cancer/software/GENE-E/) were used to generate gene lists and heat maps. Lists were mined for functional and shared gene sets using DAVID (Database for Annotation, Visualization and Integrated Discovery; Huang *et al.*, 2009a, b) and GSEA (Gene Set Enrichment Analysis) (Mootha *et al.*, 2003, Subramanian *et al.*, 2005), respectively. Verification of EMT genes was from compilations of gene sets (Groger *et al.*, 2012; Humtsoe *et al.*, 2012; Byers *et al.*, 2013). GEO accession number: GSE58393.

Transmission electron microscopy and IF transmission electron microscopy analyses

Scalp tissue was fixed and, for ImmunoTEM, incubated overnight with anti-CD133-biotin (Miltenyl, Cologne, Germany), followed by incubation with 1.4 nm streptavidin Alexa Fluor 488-fluoronanogold particles (Nanoprobes, Yaphank, NY). Tissue was refixed for electron microscopic examination, embedded in EMbed-812 (Electron Microscopy Sciences, Fort Washington, PA), and thin sections were silver enhanced with an R-Gent SE-EM kit (Electron Microscopy Sciences). Sections were examined with a JEOL 1010 electron microscope (Tokyo, Japan) fitted with a Hamamatsu digital camera (Hamamatsu City, Japan) and AMT Advantage image capture software (Danvers, MA).

Explants

Whole fetal scalp tissue was placed on a porous screen and partially submerged in DMEM/1% fetal calf serum/PS/lGlu to provide an air interface (see Figure 5a). For optimal penetration, 25 ul of anti-CD133/1 (Miltenyl) or IgG2b control antibody (diluted to 5 ug ml^{-1} in DMEM) was overlaid onto air-exposed epidermis, and another 25–30 ul was injected into the dermis. Explants were cultured at 37 °C, 5% CO_2 for 20 hours and then prepared for immunohistochemistry. An air interface technique was used because full liquid submersion resulted in dissociation of the overlying epidermis. The air interphase technique has been used successfully for other explants of tissue normally fully submerged *in vivo* (Wells *et al.*, 2010; Bull *et al.*, 2011). Others have shown that air interface can accelerate barrier development in rats (Komuves *et al.*, 1999); however, human tissue used in these studies is developmentally 8–12 weeks from this stage, and it remains unknown whether air interface might have a similar effect on human scalp development.

Statistical analyses

All statistical analyses were performed by two-tailed Student's *t*-test using Excel (Microsoft, Redmond, WA). $P<0.05$ was considered significant. All data are expressed as means ± SEM.

CONFLICT OF INTEREST

The authors state no conflict of interest.

ACKNOWLEDGMENTS

We thank the University of Pennsylvania Flow Cytometry and Cell Sorting Resource Laboratory for generous assistance with cell sorting experiments and gratefully acknowledge the assistance of J Tobias of the Penn Microarray Facility core, and S Prouty in the histology core. We especially thank Dewight Williams and Ray Meade of the Penn Electron Microscopy Resource Lab for providing valuable technical expertise and interpretation of EM results. This work was supported by National Institutes of Health grants R01-AR46837, R01-AR055309, and R21AR059346, Skin Disease Research Center grant 5-P30-AR-057217, and Edwin and Fannie Gray Hall Center for Human Appearance at University of Pennsylvania Medical Center.

SUPPLEMENTARY MATERIAL

Supplementary material is linked to the online version of the paper at http://www.nature.com/jid

REFERENCES

Abramoff MD, Magalhaes PJ, Ram SJ (2004) Image processing with ImageJ. *Biophotonics Int* 11:36–42

Anderson LH, Boulanger CA, Smith GH *et al.* (2012) Stem cell marker prominin-1 regulates branching morphogenesis, but not regenerative capacity, in the mammary gland. *Dev Dyn* 240:674–81

Andl T, Reddy ST, Gaddapara T *et al.* (2002) WNT signals are required for the initiation of hair follicle development. *Dev Cell* 2:643–53

Bolos V, Peinado H, Perez-Moreno MA *et al.* (2003) The transcription factor Slug represses E-cadherin expression and induces epithelial to mesenchymal transitions: a comparison with Snail and E47 repressors. *J Cell Sci* 116:499–511

Bull ND, Johnson TV, Welspar G *et al.* (2011) Use of an adult rat retinal explant model for screening of potential retinal ganglion cell neuroprotective therapies. *Invest Ophthalmol Vis Sci* 52:3309–20

Byers LA, Diao L, Wang J *et al.* (2013) An epithelial-mesenchymal transition gene signature predicts resistance to EGFR and PI3K inhibitors and identifies Axl as a therapeutic target for overcoming EGFR inhibitor resistance. *Clin Cancer Res* 19:279–90

Chiang C, Swan RZ, Grachtchouk M *et al.* (1999) Essential role for Sonic hedgehog during hair follicle morphogenesis. *Dev Biol* 205:1–9

Corbeil Denis (Ed) (2013) Prominin-1 (CD133): new insights on stem & cancer stem cell biology series. *Advs Exp Med Biol* 777:250,

Devenport D, Fuchs E (2008) Planar polarization in embryonic epidermis orchestrates global asymmetric morphogenesis of hair follicles. *Nat Cell Biol* 10:1257–68

Florek M, Haase M, Marzesco AM *et al.* (2005) Prominin-1/CD133, a neural and hematopoietic stem cell marker, is expressed in adult human differentiated cells and certain types of kidney cancer. *Cell Tissue Res* 319:15–26

Gay D, Kwon O, Zhang Z *et al.* (2013) Fgf9 from dermal γδ T cells induces hair follicle neogenesis after wounding. *Nat Med* 19:916–23

Groger CJ, Grubinger M, Waldhor T *et al.* (2012) Meta-analysis of gene expression signatures defining the epithelial to mesenchymal transition during cancer progression. *PLoS One* 7:e51136

Grosse-Gehling P, Fargeas CA, Dittfeld C *et al.* (2013) CD133 as a biomarker for putative cancer stem cells in solid tumours: limitations, problems and challenges. *J Pathol* 229:355–78

Heuberger J, Birchmeier W (2010) Interplay of cadherin-mediated cell adhesion and canonical Wnt signaling. *Cold Spring Harb Perspect Biol* 2:a002915

Hirata A, Utikal J, Yamashita S *et al.* (2013) Dose-dependent roles for canonical Wnt signalling in de novo crypt formation and cell cycle properties of the colonic epithelium. *Development* 140:66–75

Huang DW, Sherman BT, Lempicki RA (2009a) Systematic and integrative analysis of large gene lists using DAVID Bioinformatics Resources. *Nat Protoc* 4:44–57

Huang DW, Sherman BT, Lempicki RA (2009b) Bioinformatics enrichment tools: paths toward the comprehensive functional analysis of large gene lists. *Nucleic Acids Res.* 37:1–13

Huelsken J, Vogel R, Erdmann B *et al.* (2001) B-catenin controls hair follicle morphogenesis and stem cell differentiation in the skin. *Cell* 105:533–45

Humtsoe JO, Koya E, Pham E *et al.* (2012) Transcriptional profiling identifies upregulated genes following induction of epithelial-mesenchymal transition in squamous carcinoma cells. *Exp Cell Res* 318:379–90

Ito Y, Hamazaki TS, Ohnuma K *et al.* (2007) Isolation of murine hair-inducing cells using the cell surface marker prominin-1/CD133. *J Invest Dermatol* 127:1052–60

Jamora C, DasGupta R, Kocieniewski P *et al.* (2003) Links between signal transduction, transcription and adhesion in epithelial bud development. *Nature* 422:317–22

Jamora C, Lee P, Kocieniewski P *et al.* (2005) A signaling pathway involving TGF-beta2 and snail in hair follicle morphogenesis. *PLoS Biol* 3:e11

Karbanova J, Missol-Kolka E, Fonseca AV *et al.* (2008) The stem cell marker CD133 (prominin-1) is expressed in various human glandular epithelia. *J Histochem Cytochem* 56:977–93

Komuve L, Hanley K, Jiang Y *et al.* (1999) Induction of selected lipid metabolic enzymes and differentiation-linked structural proteins by air exposure in fetal rat skin explants. *J Invest Derm* 112:303–9

Lamouille S, Xu J, Derynck R (2014) Molecular mechanisms of epithelial-mesenchymal transition. *Nat Rev Mol Cell Biol* 15:178–96

Lee J, Tumbar T (2012) Hairy tale of signaling in hair follicle development and cycling. *Sems Cell Dev Biol* 23:906–16

Lei Z, Maeda T, Tamura A *et al.* (2012) EpCAM contributes to formation of functional tight junction in the intestinal epithelium by recruiting claudin proteins. *Dev Biol* 371:136–45

Litvinov SV, Balzar M, Winter MJ *et al.* (1997) Epithelial cell adhesion molecule (Ep-CAM) modulates cell-cell interactions mediated by classic cadherins. *J Cell Biol* 139:1337–48

Litvinov SV, Velders MP, Bakker HA (1994) Ep-CAM: a human epithelial antigen is a homophilic cell-cell adhesion molecule. *J Cell Biol* 125: 437–46

Mak AB, Nixon AM, Kittanakom S *et al.* (2012) Regulation of CD133 by HDAC6 promotes β-catenin signaling to suppress cancer cell differentiation. *Cell Rep* 2:951–63

Martínez-Estrada OM, Cullerés A, Soriano FX *et al.* (2006) The transcription factors Slug and Snail act as repressors of Claudin-1 expression in epithelial cells. *Biochem J* 394:449–57

Mikkola ML (2007) Genetic basis of skin appendage development. *Semin Cell Dev Biol* 18:225–36

Millar SE (2002) Molecular mechanisms regulating hair follicle development. *J Invest Dermatol* 118:216–25

Mootha VK, Lindgren CM, Eriksson KF *et al.* (2003) PGC-1alpha-responsive genes involved in oxidative phosphorylation are coordinately downregulated in human diabetes. *Nat Genet* 34:267–73

Müller-Röver S, Tokura Y, Welker P *et al.* (1999) E- and P-cadherin expression during murine hair follicle morphogenesis and cycling. *Exp Dermatol* 8:237–46

Nanba D, Hieda Y, Nakanishi Y (2000) Remodeling of desmosomal and hemidesmosomal adhesion systems during early morphogenesis of mouse pelage hair follicles. *J Invest Dermatol* 114:171–7

Peinado H, Olmeda D, Cano A (2007) Snail, Zeb and bHLH factors in tumour progression: an alliance against the epithelial phenotype? *Nat Rev Cancer* 7:415–28

Schneider MR, Schmidt-Ullrich R, Paus R (2009) The hair follicle as a dynamic miniorgan. *Curr Biol* 19:132–42

Shtutman M, Levina E, Ohouo P *et al.* (2006) Cell adhesion molecule L1 disrupts E-cadherin-containing adherens junctions and increases scattering and motility of MCF7 breast carcinoma cells. *Cancer Res* 66:11370–80

Stepniak E, Radice GL, Vasioukhin V (2009) Adhesive and signaling functions of cadherins and catenins in vertebrate development. *Cold Spring Harb Perspect Biol* 1:a002949

Subramanian A, Tamayo P, Mootha VK *et al.* (2005) Gene set enrichment analysis: a knowledge-based approach for interpreting genome-wide expression profiles. *Proc Natl Acad Sci USA* 102:15545–50

Surmann-Schmitt C, Widmann N, Dietz U *et al.* (2009) Wif-1 is expressed at cartilage-mesenchyme interfaces and impedes Wnt3a-mediated inhibition of chondrogenesis. *J Cell Sci* 122:3627–37

ten Berge D, Koole W, Fuerer C *et al.* (2008) Wnt signaling mediates self-organization and axis formation in embryoid bodies. *Cell Stem Cell* 3:508–18

Tinkle CL, Lechler T, Pasolli HA *et al.* (2003) Conditional targeting of E-cadherin in skin: insights into hyperproliferative and degenerative responses. *Proc Nat Acad Sci USA* 101:552–7

Tinkle CL, Pasolli HA, Stokes N *et al.* (2008) New insights into cadherin function in epidermal sheet formation and maintenance of tissue integrity. *Proc Nat Acad Sci USA* 105:15405–10

Trzpis M, Bremer E, McLaughlin PM *et al.* (2008) EpCAM in morphogenesis. *Front Biosci* 13:5050–5

Warrington SJ, Strutt H, Strutt D (2013) The Frizzled-dependent planar polarity pathway locally promotes E-cadherin turnover via recruitment of Rho-GEF2. *Development* 140:1045–54

Wells KL, Mou C, Headon DJ *et al.* (2010) Recombinant EDA or Sonic Hedgehog rescue the branching defect in ectodysplasin A pathway mutant salivary glands in vitro. *Dev Dyn* 239:2674–84

Wu CJ, Mannan P, Lu M *et al.* (2013) Epithelial cell adhesion molecule (EpCAM) regulates claudin dynamics and tight junctions. *J Biol Chem* 288:12253–68

Zhang Y, Andl T, Yang SH *et al.* (2008) Activation of beta-catenin signaling programs embryonic epidermis to hair follicle fate. *Development* 135:2161–72

Zhu L, Gibson P, Currle DS *et al.* (2009) Prominin 1 marks intestinal stem cells that are susceptible to neoplastic transformation. *Nature* 457:603–7